marine drugs

MDPI

Article

Exploration of the Electrophilic Reactivity of the Cytotoxic Marine Alkaloid Discorhabdin C and Subsequent Discovery of a New Dimeric C-1/N-13-Linked Discorhabdin Natural Product

Cary F. C. Lam, Melissa M. Cadelis and Brent R. Copp *

School of Chemical Sciences, University of Auckland, Private Bag 92019, Auckland 1142, New Zealand; clam059@aucklanduni.ac.nz (C.F.C.L.); m.cadelis@auckland.ac.nz (M.M.C.)

* Correspondence: b.copp@auckland.ac.nz

Received: 14 July 2020; Accepted: 28 July 2020; Published: 31 July 2020

Abstract: The cytotoxic marine natural product discorhabdin C contains a 2,6-dibromo-cyclohexa-2,5-diene moiety, previously proposed to be a critical feature required for biological activity. We have determined that the dienone-ring of discorhabdin C is indeed electrophilic, reacting with thiol and amine nucleophiles, affording debrominated adducts. In the case of reaction with 1-aminopentane the product contains an unusual C-2/N-18 ring closed, double-hydrate moiety. This electrophilic reactivity also extends to proteins, with lysozyme-discorhabdin C adducts being detected by ESI mass spectrometry. These results prompted further examination of an extract of discorhabdin C-producing sponge, *Latrunculia* (*Latrunculia*) *trivetricillata*, leading to the isolation and characterisation of a new example of a C-1/N-13 linked discorhabdin dimer that shared structural similarities with the 1-aminopentane-discorhabdin C adduct. To definitively assess the influence of the dienone moiety of discorhabdin C on cytotoxicity, a semi-synthetic hydrogenation derivative was prepared, affording a didebrominated ring-closed carbinolamine that was essentially devoid of tumour cell line cytotoxicity. Antiparasitic activity was assessed for a set of 14 discorhabdin alkaloids composed of natural products and semi-synthetic derivatives. Three compounds, (-)-discorhabdin L, a dimer of discorhabdin B and the discorhabdin C hydrogenation carbinolamine, exhibited pronounced activity towards *Plasmodium falciparum* K1 (IC_{50} 30–90 nM) with acceptable to excellent selectivity (selectivity index 19–510) versus a non-malignant cell line.

Keywords: marine natural product; alkaloid; discorhabdin; electrophilic reactivity; discorhabdin dimer; antimalarial

1. Introduction

Since their first report in 1987, over 40 examples of pyrroloiminoquinone alkaloids belonging to the discorhabdin/prianosin/epinardin families have been reported. Usually derived from extracts of marine sponges of the genus *Latrunculia*, these alkaloids have attracted much attention from both chemists and biologists due to their complex structures and associated biological activities [1,2]. While some of the first examples of the discorhabdins e.g., discorhabdin B (**1**) and C (**2**) (Figure 1) were structurally relatively simple [3,4], recent studies have unveiled unusual dimers [5], oligomers [6] and more complex polycyclic variants [7,8].

In many cases, discorhabdin alkaloids have been reported to exhibit cytotoxicity towards tumour cell lines [1–4,6,8,9], with additional biological activities also including inhibition of protein–protein interaction associated with hypoxia-inducible factor 1α and its transcriptional coactivator p300 [10,11], antibacterial [12–14] and antimalarial [13] properties. The biological activities

of simple dienone-containing examples of the discorhabdins has been attributed to the electrophilic properties of this moiety [2,15]. We have studied this mode of reactivity for discorhabdin B (**1**), finding that reactions with thiols including *N*-acetyl-L-cysteine affords C-1 thiol substituted C-2/N-18 ring closed analogues (e.g., **3**, Figure 2) [16] and that semi-synthetic derivatives that lack electrophilic reactivity exhibit less potent cytotoxicity. A similar conclusion was drawn from a study of *N*-13 methyl discorhabdin C (discorhabdin P) [17].

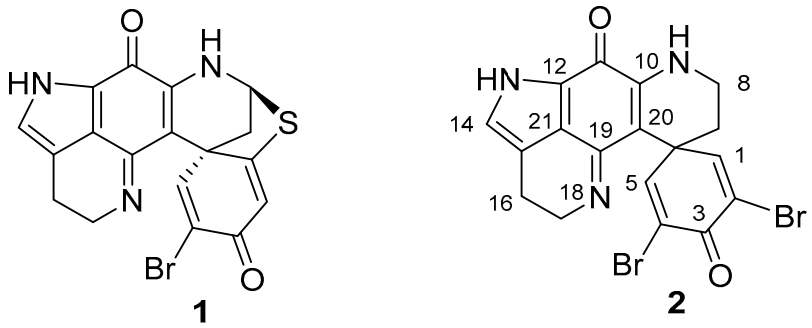

Figure 1. Structures of natural products (+)-discorhabdin B (**1**) and C (**2**).

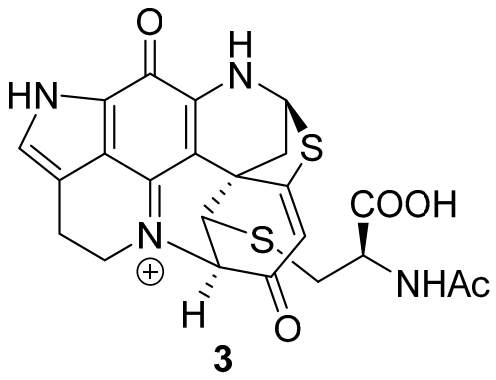

Figure 2. Structure of the *N*-acetyl-L-cysteine adduct of (+)-discorhabdin B (**3**).

As part of our ongoing interest in the discorhabdin family of alkaloids, we now examined the electrophilic reactivity of discorhabdin C towards a series of model thiol and amine nucleophiles and the amine-rich protein lysozyme, and defined the critical role played by the dieonone moiety by preparation and biological evaluation of a hydrogenated derivative of discorhabdin C. The isolation and semi-synthetic preparation of discorhabdin alkaloids with attenuated cytotoxicity (*vide infra*) provided an opportunity to discover additional biological activities for this class of natural product—screening against a panel of parasites uncovered several examples with potent and selective activity towards *Plasmodium falciparum*. During the course of this study, a new C-1/N-13 linked discorhabdin dimer was isolated from *Latrunculia (Latrunculia) trivetricillata*. Herein we report the results of these studies.

2. Results

2.1. Reactivity towards Thiols

Discorhabdin C (TFA salt) (**2**) was reacted with 1-pentanethiol (1 equiv.) in MeOH in the presence of excess triethylamine (5 equiv.) for 5 min. After this time, the dark red/black solution was directly loaded onto a C_{18} reversed-phase flash chromatography column whereby elution with H_2O + 0.05% TFA, followed by 35–40% MeOH/H_2O + 0.05% TFA afforded **4** (Figure 3) as a red solid in low (10%) yield. ESI-mass spectrometric data identified the product to be a mono-desbromo, mono-1-pentanethiol adduct, with HRESIMS protonated molecular ions observed at *m*/*z* 486.0838, corresponding to a formula

of $C_{23}H_{25}{}^{79}BrN_3O_2S$ (requires 486.0845), and *m/z* 488.0839 ($C_{23}H_{25}{}^{81}BrN_3O_2S$ requires 488.0827). ^{1}H and ^{13}C NMR data supported the structure as being a mono-thioether adduct, with direct comparison of chemical shifts with those observed for discorhabdin C identifying the site of modification as being located in the spiro-dienone fragment of the molecule. Of note were the observation of three olefinic ^{1}H singlets [δ_H 7.72 (1H, H-5), 7.21 (1H, H-14), 6.41 (1H, H-2)], changes observed for the discorhabdin C-core H_2-7 and H_2-8 resonances from triplets observed for **2** to diastereotopic multiplets in **4**, and the presence of a single unit of a 1-pentylthioether [δ_H 3.03–2.95 (H_2-2′), 1.75–1.69 (H_2-3′), 1.47–1.33 (H_2-4′ and H_2-5′) and 0.92 (H_3-6′)] (Table 1). HMBC correlations observed for H-5 (δ_H 7.72) to δ_C 176 (C-3), δ_C 126 (C-4) and δ_C 46 (C-6) also identified a new ^{13}C resonance (δ_C 170, C-1) in the spiro-dienone ring. An HMBC correlation between the pentylthioether resonances H_2-1′ (δ_H 3.03–2.95) and C-1 located the thiol substituent at C-1, completing the structure of **4**.

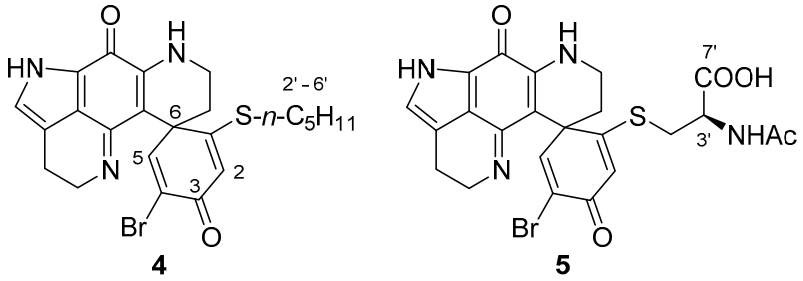

Figure 3. Structures of the 1-pentanethiol **4** and *N*-acetyl-L-cysteine adducts **5** of discorhabdin C.

Table 1. ^{1}H and ^{13}C NMR data for compounds **4** and **5** in CD_3OD (δ in ppm).

No.	4		No.	5	
	δ_H (Mult., *J* in Hz) [a]	δ_C [b]		δ_H (Mult., *J* in Hz) [c]	δ_C [d]
1	-	169.7		-	167.5
2	6.41 (s)	121.7		6.56/6.58 (s)	122.2/122.4
3	-	176.2		-	176.2
4	-	125.9		-	126.0
5	7.72 (s)	152.1		7.71 (s)	152.2
6		47.3			47.3
7	2.39–2.33 (m)	39.2/39.4		2.34 (m)	39.2/39.4
	2.16–2.12 (m)			2.13 (m)	
8	3.92–3.87 (m)	39.2/39.4		3.88 (m)	39.2/39.4
	3.73–3.67 (m)			3.69 (m)	
10	-	154.1		-	154.2
11	-	166.4		-	166.4
12	-	125.3		-	125.4
14	7.21 (s)	127.9		7.20 (s)	127.9
15		121.4		-	121.5
16	2.95–2.83 (m)	19.6		2.89 (m)	19.5
17	3.79 (t, 7.4)	45.2		3.84–3.76 (m)	45.3/45.4
19	-	156.2		-	156.1
20	-	94.8		-	94.3
21	-	124.6		-	124.6
	S-*n*-C_5H_{11}			**S-NAc-cysteine**	
2′	3.03–2.95 (m)	32.2/32.5	2′	3.54/3.57 (m)	33.8/34.2
3′	1.75–1.69 (m)	28.4		3.21/3.27 (m)	
4′	1.47–1.33 (m)	32.2/32.5	3′	4.71/4.75 (m)	51.5/52.0
5′	1.47–1.33 (m)	23.2	5′	-	173.5
6′	0.92 (t, 7.2)	14.2	6′	1.94/1.97 (s)	22.4
			7′	-	168.1

[a] 500 MHz for ^{1}H NMR; [b] 125 MHz for ^{13}C NMR; [c] 600 MHz for ^{1}H NMR; [d] 100 MHz for ^{13}C NMR.

Reaction of discorhabdin C with a second thiol nucleophile, *N*-acetyl-L-cysteine (5 equiv.) in DMF-MeOH-H_2O mixture (1:1:0.1) and trimethylamine (7 equiv.) open to the air at room temperature for 20 min gave a change of colour from bright orange to a dark orange/brown. Purification by C_{18} reversed-phase flash column chromatography [MeOH/H_2O (+0.05% TFA)] afforded the major product (**5**, 14%) as a 1:1 mixture of two diastereomers (Figure 3). HRESI mass spectrometry established a molecular formula of $C_{23}H_{22}{}^{79}BrN_4O_5S$ ($[M + H]^+$ *m/z* 545.0482, calcd. 545.0489) consistent with the product being a mono desbromo mono-*N*-acetylcysteinyl adduct of discorhabdin C. Analysis of ^1H and ^{13}C NMR data identified the presence of a single *N*-acetylcysteine residue, while the remaining resonances were almost identical to those observed for thiopentylether analogue **4** (Table 1). The observation of doubling of resonances for H-2 (δ_H 6.56 and 6.58 (s)) and for *N*-acetylcysteine resonances H_2-2′ (δ_H 3.57/3.54 and 3.27/3.21), H-3′ (δ_H 4.75 and 4.71) and *N*-Ac (δ_H 1.97 and 1.94) suggested the presence of diastereomers. The presence of diastereomeric products can be rationalised by considering that attack of the chiral nucleophile at either of the chemically equivalent C-1/C-5 spiro-dienone carbons of discorhabdin C would yield two products that are diastereomeric at C-6.

2.2. Reactivity towards Amines

The reactivity of discorhabdin C towards amine nucleophiles was investigated using 1-aminopentane and *N*α-acetyl-L-lysine. Reaction with 1-aminopentane (5 equiv.) and triethylamine (5 equiv.) in DMF for 3 h afforded a major product (31%) after purification by C_{18} reversed-phase flash chromatography. Initial ^1H NMR analysis of the product (in D_2O) indicated the sample contained at least two components, however over a 6 h period, the NMR spectrum simplified into one suggesting the presence of a single dominant compound. Analysis of 1D and 2D NMR data identified an *N*-substituted aminopentane fragment [δ_H 3.19 (2H, t, *J* = 8.0 Hz, H_2-2′), 1.74 (2H, m, H_2-3′), 1.34 (4H, m, H_2-4′,H_2-5′), 0.88 (3H, m, H_3-6′); δ_C 50.5 (C-2′), 30.6 (C-4′), 27.4 (C-3′), 24.2 (C-5′), 15.7 (C-6′)] and an intact pyrroloiminoquinone moiety [δ_H 7.22 (H-14); δ_C 122.1 (C-15), 125.7 (C-21), 126.0 (C-12)] (Table 2).

The absence of olefinic resonances due to H-1/5 identified the site of reaction to be localised at the spiro-dienone ring, while the change in appearance of both sets of methylene resonances H_2-16 and H_2-17 from clearly defined triplets (in discorhabdin C) [4] to diastereotopic multiplets suggested that the alkaloid had undergone ring closure between N-18 and C-2 [18,19]. The presence of two alkyl methines [δ_H 4.28 (d, *J* = 2.3 Hz), δ_C 55.3 (CH-1); δ_H 4.38 (d, *J* = 2.3 Hz), δ_C 66.7 (CH-2)] and the observation of an HMBC correlation between H-2 and C-19 (δ_C 154.2) further supported N-18 to C-2 ring closure. An HMBC correlation between the pentylamine H_2-2′ resonance (δ_H 3.19) and the carbon resonance at δ_C 55.3 located the amine substituent at C-1. This sequence of analysis left two protons (δ_H 4.42 and 4.15) and three ^{13}C resonances (δ_C 98.0, 75.8 and 57.5) unassigned. HSQC correlations established the resonances to be composed of two methines (δ_H 4.42, δ_C 57.5; δ_H 4.15, δ_C 75.8) and a quaternary carbon (δ_C 98.0), with a weak COSY correlation between the two protons identifying them to be part of an isolated spin-system. HMBC correlations observed for H-1 (to δ_C 41.6 (C-6)), H-2 (to δ_C 41.6 (C-6), 55.6 (C-1), 57.5 (C-4) and 98.0 (C-3)) and δ_H 4.15 (H-5) (to δ_C 41.6 (C-6), 55.6 (C-1), 57.5 (C-4) and 98.0 (C-3)) established the C-1 to C-6 spiro-ring to be entirely composed of sp^3-hydridised carbons, with C-3 (δ_C 98.0) being especially deshielded. It was interesting to note that over a period of days of being stored in D_2O NMR solvent, the signals for H-4 (δ_H 4.42) and C-4 (δ_C 57.5) would reduce in intensity, eventually disappearing from spectra. We suspected ^2H incorporation into **6** from the D_2O NMR solvent, with its attendant deuterium quadrupole relaxation, spin-spin splitting and reduced Overhauser enhancement [20], being the reasons for the loss of H-4/C-4 NMR signals. Subsequent drying of the NMR sample, followed by three cycles of dissolution in H_2O and lyophilisation then rapid re-acquisition of NMR data in either D_2O or H_2O:D_2O (9:1) restored the presence of the signals. The ESI-mass spectrum of the reaction product identified a dominant ion cluster at *m/z* 505/507, which under high resolution analysis corresponded to a molecular formula of $C_{23}H_{30}BrN_4O_4$. This formula suggested **6** was composed of a mono-debrominated discorhabdin C core bearing one aminopentane

moiety and two mole equivalents of H_2O. Additional fragment ions were observed at *m/z* 487/489 (M-H_2O) and *m/z* 469/471 (M-2H_2O), confirming the reaction product contained two moles of H_2O that were readily expelled under ESIMS conditions. ESIMS analysis of a sample dissolved in MeOH-H_2O identified an additional ion cluster at *m/z* 519/521 (M-H_2O+CH_3OH) suggesting solvent exchange with methanol was also facile. The combination of NMR chemical shifts and ESIMS data identified C-3 to be present as an acetal (δ_C 98.0) and C-5 (δ_C 75.8) was a secondary alcohol. We thus concluded the structure of the product resulting from reaction of discorhabdin C with 1-aminopentane was **6** (Figure 4).

Table 2. ^{1}H (400 MHz) and ^{13}C (100 MHz) NMR data for compound **6** in D_2O (δ in ppm) [a].

No.	δ_H (Mult., *J* in Hz)	δ_C
1	4.28 (d, 2.3)	55.3
2	4.38 (d, 2.3)	66.7
3	-	98.0
4	4.42 (d, 3.4)	57.5
5	4.15 (br m)	75.8
6		41.7
7	2.53 (d, 14.0)	25.0
	1.74 (m)	
8	3.90 (dd, 14.0, 4.3)	40.5
	3.62 (m)	
10	-	155.2
11	-	168.2
12	-	126.0
14	7.22 (s)	131.0
15		122.1
16	3.04 (m)	22.2
17	4.22 (m)	55.4
	4.06 (m)	
19	-	154.2
20	-	92.0
21	-	125.7
2′	3.19 (t, 8.0)	50.5
3′	1.74 (m)	27.4
4′	1.34 (m)	30.6
5′	1.34 (m)	24.2
6′	0.88 (m)	15.7

[a] External reference to dioxane (δ_H 3.75; δ_C 69.3).

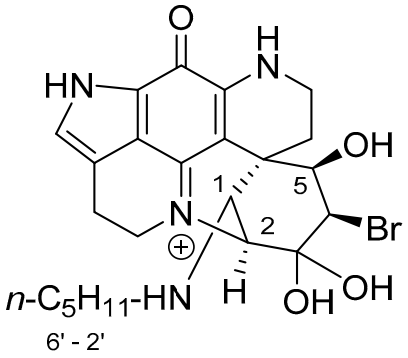

Figure 4. Structure of aminopentane discorhabdin C dihydrate adduct **6**.

With respect to the relative stereochemistry of the product, it should be noted that the geometry resulting from ring closure between N-18 and C-2 of the discorhabdin scaffold automatically defines positions C-2 and C-6 as being 2*S**,6*R** (Figure 5A,B). The configuration at positions 1 and 5 were

defined by the observation of NOESY correlations between each of H-1 (δ_H 4.28) and H-5 (δ_H 4.15) and the more downfield [16,19] of the diastereotopic methylene H_2-7 protons [H-7β (δ_H 2.53)], and from H-5 to one of the diastereotopic H_2-8 protons (H-8β, δ_H 3.62) giving configurations of 1*S** and 5*R**. Additional support for the *syn*-relationship between these three protons came from examination of the relative intensities of HMBC correlations observed in an experiment optimised for $^xJ_{CH}$ 8.33 Hz. Of the two diastereotopic H_2-7 methylene protons, δ_H 2.53 and 1.74, only the former exhibited a three-bond correlation to C-20, supporting an antiperiplanar relationship between H-7β δ_H 2.53 and C-20 [19]. The H-1 resonance (δ_H 4.28) also exhibited a strong HMBC correlation to C-20, supporting their antiperiplanar relationship. Assigning the final stereogenic centre (C-4) made use of a combination of molecular modelling, *J* analysis and NOESY data. Conformer searching using PCModel (v 10, Serena Software) identified the dominant (chair) conformers of the two diastereomers 1*S**,2*S**,4*S**,5*R**,6*R**-**6** (Figure 5A) and 1*S**,2*S**,4*R**,5*R**,6*R**-**6** (Figure 5B). The observation of a small magnitude $J_{H\text{-}4/H\text{-}5}$ coupling constant (J_{HH} = 3.4 Hz) and a NOESY correlation between the two protons was supported by model B, establishing a relative configuration of 4*R**.

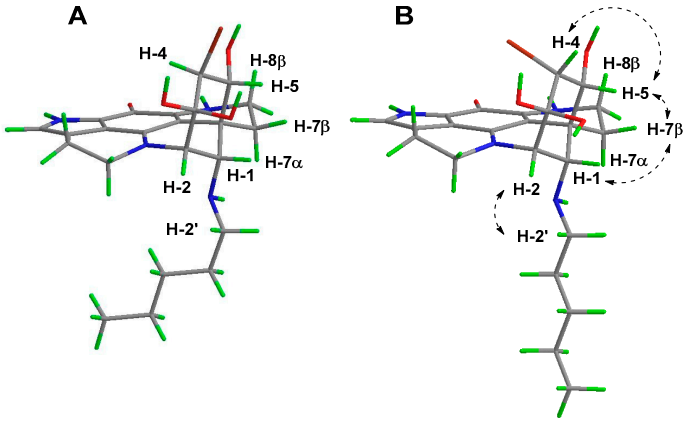

Figure 5. PCModel optimised dominant chair conformers of diastereomers 1*S**,2*S**,4*S**,5*R**,6*R**-**6** (**A**) and 1*S**,2*S**,4*R**,5*R**,6*R**-**6** (**B**) with key NOE correlations observed (**right**).

Reaction of discorhabdin C with *N*α-acetyl-L-lysine under the standard conditions yielded a complex mixture of products. Analysis by (+)-ESIMS identified the presence of ions at *m*/*z* 570.1353 (calcd. for $C_{26}H_{29}{}^{79}BrN_5O_5$, 570.1347), 588.1490 (calcd. for $C_{26}H_{31}{}^{79}BrN_5O_6$, 588.1452), 606.1546 (calcd. for $C_{26}H_{33}{}^{79}BrN_5O_7$, 606.1558) and 620.1680 (calcd. for $C_{27}H_{35}{}^{79}BrN_5O_7$, 620.1714) attributable to the formation of a mono-desbromo *N*α-acetyl-L-lysine adduct with various further additions of H_2O and CH_3OH (from MS solvent). No further characterisation of the reaction products were undertaken. In a similar manner, (+)-ESIMS analysis of the reaction of discorhabdin C with the thiol- and amine-containing nucleophile glutathione (5 equiv.) identified an extensive array of ions at *m*/*z* 689.1028/691.1013 ($C_{28}H_{30}BrN_6O_8S$), 725.1219/727.1196 ($C_{28}H_{34}BrN_6O_{10}S$) and 739.1402/741.1371 ($C_{29}H_{36}BrN_6O_{10}S$) consistent with the presence of *N*-/*S*-glutathionyl and H_2O/CH_3OH adducts.

2.3. Reaction with Lysozyme

The successful demonstration that discorhabdin C reacts with model amine nucleophiles prompted us to next investigate reactivity towards the lysine-rich model protein lysozyme using (+)-ESIMS to identify the presence of any reaction products [21]. Incubation of discorhabdin C with hen egg white lysozyme (HEWL) in H_2O for 12 h gave no detectable adducts, but by day 3, two peaks representing mass additions of +382 mu (2%) and +418 mu (1%) were detected. These adducts are likely the result of the reaction of lysine residues in the protein with discorhabdin C, with the higher mass adduct corresponding to further addition of two equivalents of H_2O, fully consistent with the 1-aminopentane adduct study.

2.4. A Cyclic Carbinolamine Analogue of Discorhabdin C

Collectively these studies characterise the electrophilic reactivity of the spiro-dienone moiety of discorhabdin C, a structural feature that is known to be a factor, but not the sole determinant, for the cytotoxicity reported for this class of alkaloid [15–17]. To further explore the degree of essentiality of the dienone ring towards cytotoxicity, discorhabdin C was subjected to hydrogenation using Pd/C under an H_2 atmosphere for 15 min to afford, after workup, a blue-coloured product in 71% yield. HR ESI mass spectrometry determined a formula of $C_{18}H_{20}N_3O_2$ ([M] + 310.1542, calcd. 310.1550) indicating didebromination and addition of two moles of H_2. Direct comparison with ^{1}H NMR data observed for discorhabdin C [4] identified the absence of H-1/5 olefinic resonances, a downfield shift for H_2-17 ($\Delta\delta$ +0.38), upfield shifts for H_2-8 ($\Delta\delta$ –0.24), and H_2-7 ($\Delta\delta$ –0.41) and the presence of two new signals at 2.28–2.14 (m) and 1.85, with the latter two signals integrating for 4H each (Table 3). Comparison of ^{13}C and HSQC 2D NMR data revealed the absence of resonances associated with the dienone moiety of **2** and the presence of new signals attributable to two chemically equivalent methylenes (δ_H 2.28–2.14, δ_C 35.9; δ_H 1.85, δ_C33.8) and a deshielded ^{13}C quaternary resonance at δ_C 92.0. HMBC correlations from H_2-1/5 (δ_H 1.85), H_2-2/4 (δ_H 2.28-2.14) and H_2-17 (δ_H 4.15) to the resonance at δ_C 92.0 located the carbon at C-3 and also established ring closure between C-3 and N-18. In this manner the structure of the reaction product was concluded to be the cyclic carbinolamine **7** (Figure 6).

Table 3. ^{1}H (400 MHz) and ^{13}C (100 MHz) NMR data for compound **7** in CD_3OD (δ in ppm).

No.	δ_H (Mult., *J* in Hz)	δ_C
1	1.85 (t, 7.2)	33.8
2	2.28–2.14 (m)	35.9
3	-	92.0
4	2.28–2.14 (m)	35.9
5	1.85 (t, 7.2)	33.8
6	-	35.1
7	1.68 (t, 5.5)	36.2
8	3.46 (t, 5.5)	39.1
10	-	151.4
11	-	167.7
12	-	124.8
14	7.10 (s)	126.5
15	-	121.2
16	2.91 (t, 7.1)	21.1
17	4.15 (t, 7.1)	45.8
19	-	157.1
20	-	106.4
21	-	125.4

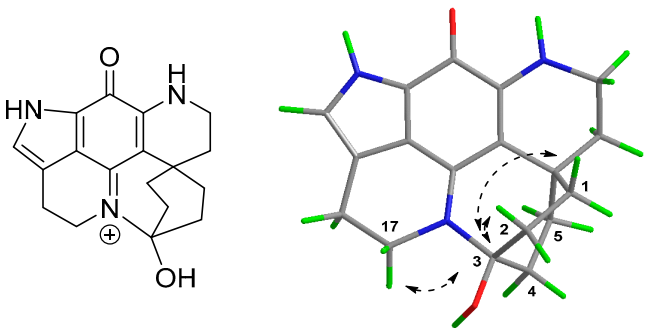

Figure 6. Structure of carbinolamine analogue of discorhabdin C **7** (**left**) and key HMBC correlations supporting the ring-closed structure (**right**).

2.5. Isolation of a New Example of a C-N-Linked Discorhabdin Dimer

Having established the electrophilic reactivity of discorhabdin C, we were prompted to re-examine chromatographic fractions obtained from Latrunculia (Latrunculia) trivetricillata, the marine sponge source of discorhabdin C used in the present study. Non-purple fractions (i.e., those not containing discorhabdin C) obtained by LH-20 chromatography of the crude sponge extract were subjected to ^{1}H NMR and ESIMS-directed fractionation using combinations of LH-20 and C_{18} reversed-phase column chromatography to afford **8** as a brown non-crystalline solid. Analysis of the (+)-HRESI mass spectrum of **8** identified molecular ions at m/z 879/881/883/885, with the corresponding protonated doubly charged ions at m/z 440/441/442/443 also observed. The assigned molecular formula of $C_{36}H_{30}Br_3N_6O_6$ suggested the presence of a pseudo-dimer composed of two discorhabdin C-like fragments [6]. Interpretation of 1D and 2D NMR data revealed the presence of two distinct discorhabdin scaffolds, one of which was very similar to discorhabdin C ('fragment A'), and the second ('fragment B') very similar to the keto-hydrate structure of aminopentane adduct **6**.

The NMR resonances observed for fragment A were similar to those observed for discorhabdin C, particularly with respect to ^{1}H resonances associated with the spiro-dienone moiety [H-1/H-5 (δ_H 7.81 (s)), H_2-7 (δ_H 2.15), and H_2-8 (δ_H 3.76)] [4] (Table 4). In contrast, resonances associated H-14 (δ_H 6.86) and H_2-16 (δ_H 2.72) of the iminoquinone core of the fragment were different (more shielded) when compared to the corresponding resonances in discorhabdin C, suggesting the presence of a substituent at the N-13 position of discorhabdin C. Investigation of the second set (fragment B) of resonances revealed a familiar structure, with ^{1}H NMR resonances attributable to a ring closed (C-2′ N-18′), keto-hydrate discorhabdin-like structure, as observed for aminopentane adduct **6**. Resonances associated with the C-1′ to C-6′ ring of **8** were assigned by analysis of NMR data obtained in D_2O and ^{1}H and ^{13}C NMR 1D spectra acquired in 9/1 H_2O/D_2O. Similar to **6**, a fragment sequence of C-1′ (δ_H 6.44; δc 54.1), C-2′ (δ_H 4.29; δc 71.2); C-3′ (δc 98.4), C-4′ (δ_H obscured; δc 58.6), C-5′ (δ_H 4.16; δc 76.0) to C-6′ (δc 42.8) was established using a combination of COSY, HSQC and HMBC NMR data. Of particular note was the unusually deshielded resonance observed for H-1′ (δ_H 6.44), identifying the presence of a highly electron withdrawing group at C-1′ [6]. Other proton spin-system resonances associated with fragment B were found to be almost identical to those observed for aminopentane adduct **6** including resonances for H_2-7′ (δ_H 2.31, 1.07), H_2-8′ (δ_H 3.89, 3.56), H-14′ (δ_H 7.24), H_2-16′ (δ_H 3.06) and H_2-17′ (δ_H 4.13, 4.04). Connectivity between the two fragments was revealed by the observation of HMBC correlations from H-1′ (δ_H 6.44) to both C-12 (δ_C 126.6) and C-14 (δ_C 130.1), establishing **8** to be a new example of a C-1′/N-13 linked discorhabdin dimer [6].

The relative configuration of stereogenic centres in **8** were established by interpretation of NOESY correlations, in combination with qualitative analysis of ^{1}H-^{13}C dihedral angles derived from the strength of HMBC NMR correlations. The first step was to again note that C-2/N-18 ring closure defines the scaffold configuration as 2′*S**, 6′*R**. Unfortunately only a limited number of NOESY correlations were observed for signals in the C-1 to C-6 fragment, namely H-1′ (δ_H 6.44) to one of the diastereotopic methylene protons at H_2-7′ (δ_H 2.31), and from H-5′ (δ_H 4.17) to one of the diastereotopic methylene protons at H_2-8′ (δ_H 3.56). Differentiating between the H_2-7′ methylene protons (δ_H 2.31, 1.07) as either α (axial) or β (equatorial) was achieved by examination of the intensity of 3-bond ^{1}H-^{13}C HMBC correlations, in a similar manner to that used earlier for adduct **6**. Of the methylene two protons, only one of them (δ_H 1.07) exhibited a strong correlation to C-5′ (δ_C 76.0) in an HMBC experiment optimised to $^{x}J_{CH}$ 8.33 Hz. As only the α-faced (axial) proton is in an antiperiplanar geometry with C-5′ (PCModel conformer search and optimised geometry, Figure 7), the methylene resonance at δ_H 1.07 was attributed to H-7′α, leaving the remaining H-7′ resonance at δ_H 2.31 as the 7′β (equatorial) proton [19]. Thus, the observation of a NOESY correlation from H-1′ to H-7′β defined configuration at C-1′ as *S**. No useful NOESY correlations were observed for H-5′, however the similarity of chemical shifts and J_{HH} coupling constants for H-2/H-4 and H-5 of both **6** and **8** gave us confidence to assign similar relative configuration to **8**, i.e., 1*S**,2*S**,4*R**,5*R**,6*R** (Figure 7). Strong inter-fragment NOESY correlations were observed between H-14 in fragment A and H-2′′ (δ_H 4.28), H-7′α (δ_H 1.07) and H_2-17′

(H-17′α, δ_H 4.00) in fragment B, providing further evidence for the C-1α (axial) orientation of the N-13 substituted discorhabdin C fragment A (Figure 7). No specific rotation nor circular dichroism Cotton Effects were observed at any wavelengths, identifying that **8** had been isolated as the racemate.

Table 4. ^{1}H (400 MHz) and ^{13}C (100 MHz) NMR data for compound **8** (δ in ppm).

No.	δ_H (Mult., *J* in Hz) [a]	δ_C [b]	No.	δ_H (Mult., *J* in Hz) [a]	δ_C [b]
1	7.81 (s)	156.0	1′	6.44 (d, 2.0)	54.1
2	-	124.9	2′	4.29 (d, 2.0)	71.2
3	-	177.0	3′	-	98.4
4	-	124.9	4′	Obscured	58.6
5	7.81 (s)	156.0	5′	4.16 (br m)	76.0
6	-	47.7	6′	-	42.8
7	2.15 (t, 5.5)	35.3	7′	2.31 (dd, 13.5, 2.4)	24.3
8	3.76 (m)	41.1		1.07 (td, 13.5, 5.4)	
10	-	154.9	8′	3.89 (m)	40.6
11	-	169.6		3.56 (m)	
12	-	126.6	10′	-	154.9
14	6.86 (s)	130.1	11′	-	168.8
15	-	124.5	12′	-	125.5/126.2
16	2.72 (m)	20.7	14′	7.24 (s)	130.8
17	3.89 (m)	46.6	15′	-	122.3
19	-	156.5	16′	3.06 (m)	22.2
20	-	93.7/94.0	17′	4.13 (m)	55.4
21	-	126.6		4.04 (m)	
			19′	-	154.2
			20′	-	93.7/94.0
			21′	-	125.5/126.2

[a] D_2O; [b] 90% H_2O + 10% D_2O. Both sets of data externally reference to dioxane (δ_H 3.75; δ_C 69.3).

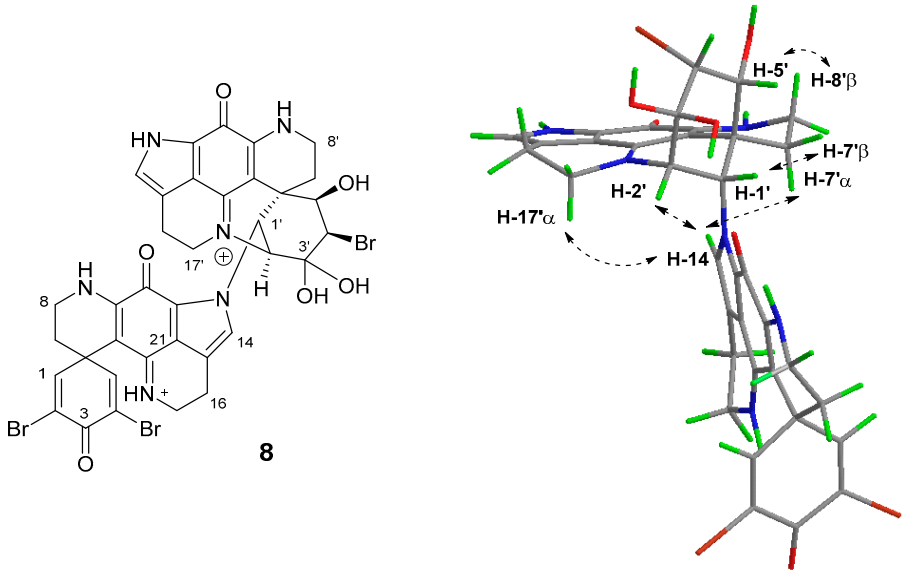

Figure 7. The structure of discorhabdin C dimer (**8**) (**left**) and key intra- (H-1′/H-7′β, H-5′/H-8′β) and inter-fragment (between H-14 (of fragment A) and H-17′α, H-2′ and H-7′α (of fragment B)) NOESY correlations (**right**) observed.

To examine the possibility of this natural product being an artefact produced during isolation, samples of free base discorhabdin C were left to stir in the presence of TEA and water. Reaction was monitored by HPLC at 12 h intervals, with no significant change observed. The reaction was halted

after 48 h, which yielded small quantities of discorhabdin C and a decomposed mixture, analysis of which did not indicate the presence of any dimer-related products.

2.6. Assessing Biological Activities

Discorhabdin C (**2**) and analogues **4**, **6** and **7** were evaluated for cytotoxicity towards a panel of human tumour cell lines as part of the Developmental Therapeutics Program of the National Cancer Institute. Unfortunately, due to compound instability, dimer **8** was not submitted for testing. The thiopentanyl analogue **4** was found to be approximately an order of magnitude less active than the parent alkaloid discorhabdin C (Table 5). Of note was that analogues **6** (NSC 791238) and **7** (NSC 791237), both of which lack any dienone functionality, were deemed inactive in preliminary single dose (10 μM) testing, with tumour cell mean growth values of 100.67% (delta 33.70, range 63.59) and 99.57% (delta 37.53, range 59.64), respectively. Neither compound was progressed to determination of GI_{50}/TGI/LC_{50} values. The results for these latter two semi-synthetic derivatives provides direct support for the critical role played by the spiro-dienone ring in the cytotoxic properties of discorhabdin C.

Table 5. In vitro antitumour activities (μM) of discorhabdin C (**2**) and thiopentanyl analogue **4.**

Compound (NSC) [1]	GI_{50} [2]	TGI [2]	LC_{50} [2]
2 (626162)	0.13	0.36	2.3
4 (789237)	1.4	3.9	10.5

[1] NSC number is the NCI reference number for each compound. Search for this number at http://dtp.cancer.gov to view complete information of all in vitro assay profiles; [2] GI_{50} (50% growth inhibition), TGI (total growth inhibition) and LC_{50} (50% cell kill) data are averaged calculated mean micro-molar values obtained from two experiments at the NCI.

Natural products containing the iminoquinone scaffold have been reported to exhibit antimalarial activity, including discorhabdin C, which was active (*Plasmodium falciparum* (*Pf*) D6 clone IC_{50} 2.8 μM, *Pf* W2 clone IC_{50} 2.0 μM) but with negligible selectivity (Vero cell line IC_{50} 2.8 μM), and 3-dihydrodiscorhabdin C (**9**) (Figure 8) with strong and selective anti-*Pf* activity (D6 IC_{50} 0.17 μM, *Pf* W2 IC_{50} 0.13 μM, Vero IC_{50} 9.8 μM) [13]. The structurally-simpler alkaloids tsitsikammamine C and makaluvamines J, G and L, each of which lack a spiro-dienone moiety, exhibited pronounced in vitro activity towards *Pf* clones 3D7 and Dd2 (IC_{50} 13–40 nM), with only negligible cytotoxicity towards the HEK293 cell line (IC_{50} 1.2–3.6 μM) [22]. Together these results prompted us to evaluate the antiparasitic activities of a series of discorhabdin natural products and semi-synthetic analogues that we have previously shown to exhibit modest or minimal tumour cell line cytotoxicity. Included in this study were (+)-discorhabdin B **1**, discorhabdin C **2**, **6**–**8**, 3-dihydrodiscorhabdin C **9** [15], (+)-discorhabdin D **10**, (-)-discorhabdin H **11**, (+)-discorhabdin H_2 **12** [19] (-)-discorhabdin L **13**, discorhabdin Q **14**, discorhabdin U **15**, semi-synthetic dienone-phenol **16** [23] and discorhabdin B dimer **17** [5,16] (Figure 8).

The set of compounds were screened against a panel of four parasitic protozoa: *Trypanosoma brucei rhodesiense*, *Trypanosoma cruzi*, *Leishmania donovani* and *Plasmodium falciparum* K1 dual drug-resistant strain. Initial testing was part of a larger library medium-throughput-screen, using two set doses (4.81 and 0.81 μg/mL). Compounds that exhibited some degree of selectivity (i.e., were not strongly active against three or four parasites which was considered a sign of general toxicity) were then evaluated for IC_{50} against the parasites and for cytotoxicity towards the L6 rat myoblast cell line (Table 6).

All compounds exhibited some degree of antimalarial activity, with natural product (-)-discorhabdin L (**13**) and semi-synthetic analogues **7** and **17** being particularly potent (IC_{50} 30, 90 and 80 nM, respectively) and selective versus the L6 mammalian cell line (SI 37, 19 and 510, respectively). Additionally, also of note were the sub-micromolar activities of **8**, **13** and **17** towards *Trypanosoma brucei rhodesiense*. In the case of discorhabdin B dimer **17**, it is interesting to contrast the low cytotoxicity towards the non-malignant rat skeletal myoblast cell line L6 (IC_{50} 41 μM) (Table 6), compared to the recently reported strong cytotoxicity observed for the same compound towards a

human colon tumour cell line HCT-116 (IC_{50} 0.16 μM) and a non-malignant human keratinocyte cell line (IC_{50} 0.56 μM) [5].

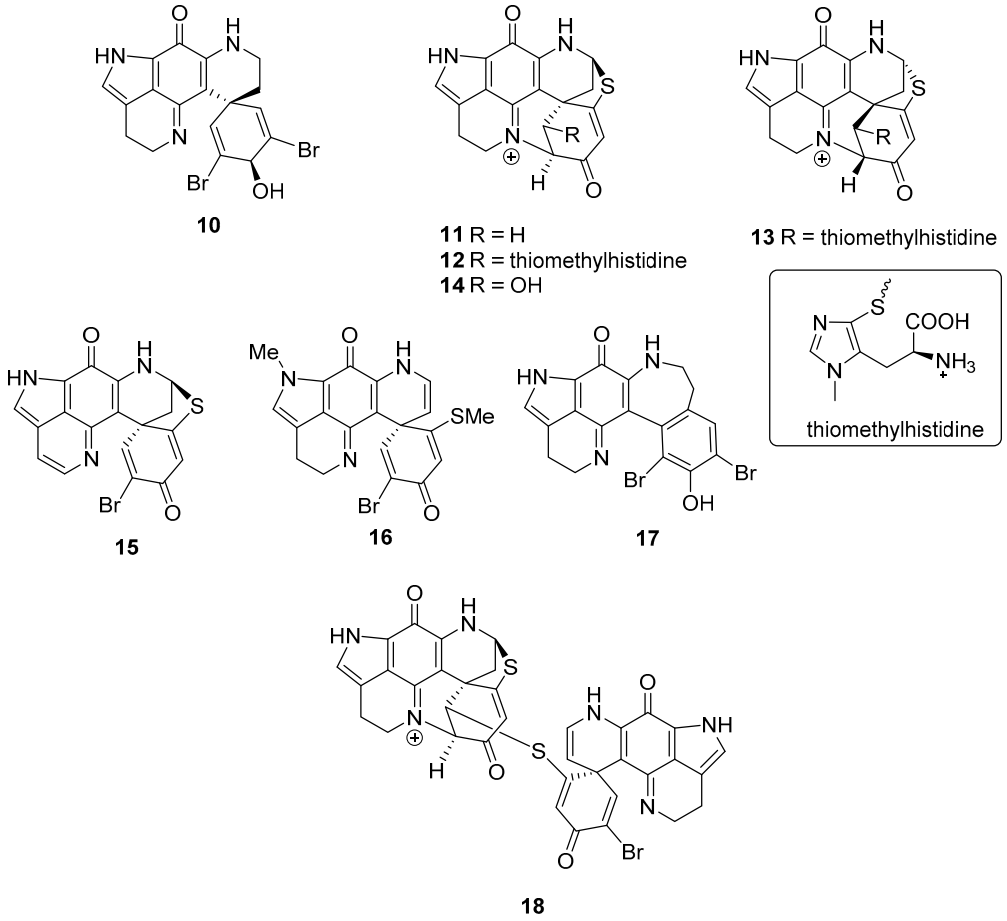

Figure 8. Structures of additional discorhabdin natural product and semi-synthetic analogues **9**–**17** that were evaluated for antiparasitic and cytotoxic properties.

Table 6. Anti-protozoal and cytotoxic activities of discorhabdin natural products and semisynthetic analogues **1**, **2**, **6**–**17**.

Compd.	*T. B. Rhod.*[b]	*T. Cruzi*[c]	*L. Don.*[d]	*P. Falc.* K1 [e]	L6 [f]	SI *Pf* [g]
1	99% (1.5)	100% (1.5)	57% (1.5)	100% (1.5)	n.t. [h]	-
2	99% (1.4)	100% (1.4)	47% (1.4)	100% (1.4)	n.t.	-
6	n.t.	n.t.	n.t.	0.25	0.81	3.2
7	n.t.	n.t.	n.t.	0.09	1.7	19
8	0.71	11.1	18.7	6.4	2.1	0.3
9	n.t.	n.t.	n.t.	0.40	0.11	0.3
10	99% (1.8)	100% (1.8)	75% (1.8)	100% (1.8)	n.t.	-
11	1.4	29	64	1.6	9.1	5.7
12	2.3	63	94	12	17	1.4
13	0.40	3.6	7.2	0.03	1.1	37
14	1.3	9% (12)	20% (1.9)	20% (1.9)	11	-
15	100% (1.5)	100% (1.5)	97% (1.5)	100% (1.5)	n.t.	-
16	n.t.	n.t.	n.t.	1.7	6.1	3.6
17	0.33	0% (0.8)	29% (0.8)	0.08	41	510

[a] IC_{50} values in μM, or % inhibition at the μM dose stated. All data is the mean value from duplicate assays; [b] *Trypanosoma brucei rhodesiense* (positive control melarsoprol, IC_{50} 0.01 μM); [c] *Trypanosoma cruzi* (positive control benznidazole, IC_{50} 1.35 μM); [d] *Leishmania donovani* (positive control miltefosine, IC_{50} 0.52 μM); [e] *Plasmodium falciparum*, K1 strain (positive control chloroquine, IC_{50} 0.20 μM); [f] L6 rat skeletal myoblast cell line for cytotoxicity (positive control podophyllotoxin, IC_{50} 0.01 μM); [g] Antiplasmodial selectivity index = L6 IC_{50}/P f. IC_{50}; [h] Not tested.

3. Discussion

In an effort to understand the potential role played by the spiro-(di)enone moiety in the cytotoxicity of discorhabdin alkaloids, we have previously investigated the electrophilic reactivity of discorhabdin B towards biomimetic nucleophiles [16] and prepared semi-synthetic analogues of discorhabdin P [17]. Collectively these studies concluded that electrophilic reactivity was a major, though not exclusive, source of alkaloid cytotoxicity. In the present study, we examined the reactivity of discorhabdin C, using similar methodology of determining reactivity toward nucleophiles and the cytotoxic evaluation of a semi-synthetic analogue that lacks the dibromo-dienone 'warhead' [23]. Interestingly when compared with discorhabdin B reactivity, the results observed for discorhabdin C are quite distinct. While both compounds reacted with thiol nucleophiles, the structures of the products were noticeably different with (+)-discorhabdin B (**1**) yielding a C-1 thiol-substituted compound that also embodied a C-2/N-18 ring closure (e.g., **3**) with discorhabdin C (**2**) reacting to afford thiol-substituted spiro-dienones **4** and **5** (Figure 9). Presumably the thioether group present in the natural product **1**, but absent in **2**, provides enough distortion to the geometry of the spiro-dienone ring to facilitate ring closure to yield **3**. In direct contrast however were the results of reaction of **1** and **2** with amine-containing nucleophiles. While the reaction of (+)-discorhabdin B with amine nucleophiles yielded intractable mixtures and natural product decomposition [16], discorhabdin C afforded a product from reaction with 1-aminopentane that embodied C-1 attack and C-2/N-18 ring closure. From such a sequence of steps, one would expect the product to contain an enone moiety: in the case of **6** however, the end product, when characterised in aqueous solvent, was the result of further addition of two mole equivalents of water. These results prompted us to re-examine extracts of the discorhabdin C-producing sponge (*Latrunculia* (*Latrunculia*) *trivetricillata*) used in the current study, leading to the isolation and characterisation of a new discorhabdin dimer **8**. The structure is closely related to discorhabdin B oligomers recently reported from a deep sea collection of *Latrunculia biformis* [6] with all examples featuring a C-1/N-13 linkage between discorhabdin fragments. It is interesting to note that while the di- and tri-discorhabdin structures contained a β-configuration (equatorial) C-1/N-13 connection and the trimer exhibited potent cytotoxicity towards the HCT-116 cell line (IC_{50} 0.31 μM), dimer **8** contained an α-configuration (axial) linkage and was only weakly cytotoxic to the L6 rat myoblast cell line (IC_{50} 2.1 μM).

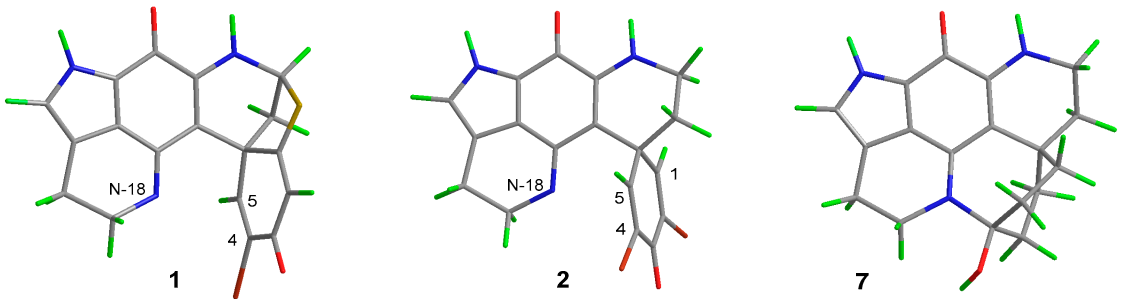

Figure 9. Summary of electrophilic reactivity/cytotoxicity observed for discorhabdin B (**1**) [16] and discorhabdin C (**2**) and cyclic carbinolamine derivative (**7**) (present study).

One of our goals of seeking clarity on the contribution of the spiro-dienone ring to the observed biological activity (cytotoxicity) of discorhabdin C was achieved by semi-synthesis of carbinolamine **7**. $Pd/C/H_2$ hydrogenation of discorhabdin C was expected to yield a desbromo-spiro-cyclohexanone product which was anticipated to be incapable of electrophilic reactivity and hence to exhibit attenuated cytotoxicity. Indeed, the product, which was characterised as the ring-closed C-3/N-18 carbinolamine,

was found to be devoid of antitumour activity when tested against the human 60 cell-line panel at the NCI (Figure 9). Non- or poorly cytotoxic discorhabdin analogues were also shown to exhibit favourable levels of antimalarial activity, opening a further avenue for investigation of this renowned class of marine natural products.

4. Materials and Methods

4.1. General Experimental Procedures

Infrared spectra were recorded on a Perkin-Elmer spectrometer 100 Fourier Transform infrared spectrometer equipped with a universal ATR accessory (PerkinElmer, Boston, MA, USA). Mass spectra were acquired on a Bruker micrOTOF Q II spectrometer (Bruker®, Billerica, MA, USA). NMR spectra were recorded at 298 K on Bruker AVANCE 400, 500 and 600 spectrometers (Bruker®, Billerica, MA, USA) using standard pulse sequences. Proto-deutero solvent signals were used as internal references (CD_3OD: δ_H 3.30, δ_C 49.00) or in the case of D_2O or H_2O/D_2O mixtures, dioxane was used as an external reference (δ_H 3.75; δ_C 69.3). For ^1H NMR, the data are quoted as position (δ), relative integral, multiplicity (s = singlet, d = doublet, t = triplet, q = quartet, m = multiplet, br = broad), coupling constant (*J*, Hz), and assignment to the atom. The ^{13}C NMR data are quoted as position (δ), and assignment to the atom. The original spectra of the relative compounds could be found in Supplementary Materials. Flash column chromatography was carried out using Merck (Manukau, Auckland) LiChroPrep C_{18} reversed-phase (40–63 or 25–40 μm) solid support. Thin layer chromatography was conducted on Merck DC-plastikfolien Kieselgel 60 F254 or on Merck DC Kieselgel 60 RP-18 F254S plates. Analytical reversed-phase HPLC was run on a Waters 600 HPLC photodiode array system (Milford, MA, USA) using an Alltech C_8 column (3 μm Econosphere Rocket, 7 × 33 mm) (Grace, Columbia, MA, USA) and eluting with a linear gradient of H_2O (0.05% TFA) to MeCN over 13.5 min at 2 mL/min. All solvents used were of analytical grade or better and/or purified according to standard procedures. Chemical reagents used were purchased from standard chemical suppliers and used as purchased. Samples of discorhabdin C used in this study were isolated from specimens of *Latrunculia* (*Latrunculia*) *trivetricillata* (MNP 6116) collected from the Three Kings Islands, New Zealand using protocols previously reported [19]. Antitumour cell lines were sourced from the DCTD Tumor repository, National Cancer Institute at Frederick, Maryland USA. Strains of *T. B. rhodesiense*, *T. cruzi*, *L. donovani* and *P. falciparum* were obtained from Swiss Tropical and Public Health Institute.

4.2. Semi-Synthesis

4.2.1. Thiopentanyl-Discorhabdin C Adduct (**4**)

To a solution of discorhabdin C trifluoroacetate salt (0.045 g, 0.1 mmol) in MeOH (1 mL) was added triethylamine (0.049 g, 0.5 mmol) followed by 1-pentanethiol (0.010 g, 0.1 mmol). The reaction mixture was stirred for 5 min before being directly loading onto a reversed-phase C_{18} chromatography column and washed with three column volumes of H_2O (+0.05% TFA). Elution with 35–40% aq. MeOH (+0.05% TFA) afforded **4** as a red-purple non-crystalline trifluoroacetate salt (5.0 mg, 10%). R_f (CH_2Cl_2/MeOH, 9:1) 0.57; IR (ATR) ν_{max} 3381, 1679, 1204, 1136 cm^{-1}; ^1H NMR (CD_3OD, 500 MHz) and ^{13}C NMR (CD_3OD, 125 MHz) Table 1; (+)-HRESIMS $[M+H]^+$ *m/z* 486.0838 (calcd. for $C_{23}H_{25}{}^{79}BrN_3O_2S$, 486.0845), 488.0839 (calcd. for $C_{23}H_{25}{}^{81}BrN_3O_2S$, 488.0827).

4.2.2. *N*-Acetyl-L-Cysteinyl Discorhabdin C Adduct (**5**)

N-Acetyl-L-cysteine (26 mg, 0.16 mmol) was dissolved in DMF (0.5 mL), MeOH (1 mL) and water (0.1 mL), followed by addition of TEA (23 μL, 0.16 mmol). Free base discorhabdin C (15.0 mg, 32.0 μmol) was dissolved in DMF (0.5 mL), followed by addition of TEA (9 μL, 64 μmol) and the *N*-acetyl-L-cysteine mixture. The reaction mixture was stirred in air for 30 min before loading the reaction mixture directly onto a reversed-phase C_{18} chromatography column and washed with three column volumes of water

(0.05% TFA). Elution with 10% MeOH (0.05% TFA) yielded a brown fraction which was further purified using C_{18} (25–40 μm) column chromatography eluting with 10% MeOH in H_2O (0.05% TFA) to afford a mixture of diastereomers (1:1) **5** (3.0 mg, 14%) as purple non-crystalline trifluoroacetate salts. R_T 4.48 min; IR (ATR) 3267, 1673, 1545, 1200 cm^{-1}; ^1H NMR (CD_3OD, 600 MHz) and ^{13}C NMR (CD_3OD, 100 MHz) Table 1; (+)-HRESIMS *m/z* $[M+H]^+$ 545.0482 (calcd. for $C_{23}H_{22}{}^{79}BrN_4O_5S$, 545.0489), 547.0468 (calcd. for $C_{23}H_{22}{}^{81}Br_2N_4O_5S$, 547.0469). Resonances for C-3′ were obtained indirectly from HSQC NMR data.

4.2.3. Aminopentane Discorhabdin C Dihydrate Adduct (**6**)

A solution of 1-aminopentane (12 μL, 0.12 mmol), DMF (2 mL) and TEA (18 μL, 0.13 mmol) was added to discorhabdin C trifluoroacetate salt (12.0 mg, 0.021 mmol). The reaction mixture was stirred in air for 3 h before being loaded directly onto a reversed-phase C_{18} chromatography column and washing with three column volumes of water (0.05% TFA). The first purple fraction eluted at 10% MeOH (0.05% TFA) was collected and dried in vacuo, before re-dissolving in H_2O. After 12 h, the sample was dried in vacuo to yield compound **6** (4.0 mg, 31%) as a purple non-crystalline trifluoroacetate salt. R_T 3.10 min; IR (ATR) 3195, 1669, 1541, 1198, 1135 cm^{-1}; ^1H NMR (D_2O, 400 MHz) and ^{13}C NMR (D_2O, 100 MHz) Table 2; (+)-HRESIMS *m/z* $[M]^+$ 469.1220 (calcd. for $C_{23}H_{26}{}^{79}BrN_4O_2$, 469.1234), 471.1205 (calcd. for $C_{23}H_{26}{}^{81}BrN_4O_2$, 471.1214), 487.1313 (calcd. for $C_{23}H_{28}{}^{79}BrN_4O_3$, 487.1339), 489.1307 (calcd. for $C_{23}H_{28}{}^{81}BrN_4O_3$, 489.1320), 505.1438 (calcd. for $C_{23}H_{30}{}^{79}BrN_4O_4$, 505.1445), 507.1419 (calcd. for $C_{23}H_{30}{}^{81}BrN_4O_4$, 507.1426), 519.1594 (calcd. for $C_{24}H_{32}{}^{79}BrN_4O_4$, 519.1601), 521.1568 (calcd. for $C_{24}H_{32}{}^{81}BrN_4O_4$, 521.1582).

4.2.4. Discorhabdin C Hydrogenation Product (**7**)

Discorhabdin C (**2**) as the trifluoroacetate salt (8.00 mg, 13.9 μmol) was dissolved in dry MeOH (4 mL), followed by addition of a spatula tip of Pd/C (10%). The reaction mixture was purged under H_2 and stirred at r.t. for 15 min. The crude reaction product was filtered through a cotton wool plug, and the solvent removed in vacuo. Purification using reversed-phase C_{18} flash column chromatography (10% to 25% MeOH/H_2O + 0.05% TFA) afforded **7** as a blue non-crystalline trifluoroacetate salt (4.20 mg, 71%). R_f (30% (10% aq. HCl) 0.68, 70% MeOH); IR (ATR) 3390, 3239, 1671, 1194, 1173, 1126 cm^{-1}; ^1H NMR (CD_3OD, 400 MHz) and ^{13}C NMR (CD_3OD, 100 MHz) Table 3; (+)-HRESIMS *m/z* $[M]^+$ 310.1542 (calcd. for $C_{18}H_{20}N_3O_2$, 310.1550).

*4.3. Isolation and Purification of Discorhabdin C (**2**) and Dimer (**8**)*

Freeze dried *Latrunculia* (*Latrunculia*) *trivetricillata* sponge material (7.3 g) was extracted with MeOH (4 × 250 mL). The solvent was filtered and then removed in vacuo to give a purple/brown crude extract (1.62 g). The crude extract was subjected to Sephadex LH-20 (MeOH (0.05% TFA)) column chromatography to afford brown- and purple-coloured fractions. The brown fraction was further purified with Sephadex LH-20 (MeOH (0.05% TFA)), followed by reversed-phase C_{18} column chromatography (10% MeOH/H_2O (0.05% TFA)) to give dimer **8** as a brown non-crystalline trifluoroacetate salt (9.5 mg, 0.13%, dry weight). Further purification of the purple fraction using reversed-phase C_{18} column chromatography (10% MeOH/H_2O (0.05% TFA)) afforded discorhabdin C (**2**) (155.5 mg, 2.13% dry weight), spectroscopic data for which matched literature values [4].

Dimer **8**: R_T 5.57 min; IR (ATR) 3261, 1676, 1541, 1202, 1134 cm^{-1}; UV-Vis (MeOH) λ_{max} (log ε) 250 (4.49), 366 (4.15), 396 sh (4.08), 545 (3.22) nm; ^1H NMR (D_2O, 400 MHz) and ^{13}C NMR (90% H_2O + 10% D_2O, 100 MHz) Table 4; (+)-HRESIMS m/z $[M]^+$ 878.9782 (calcd. for $C_{36}H_{30}{}^{79}Br_3N_6O_6$, 878.9771), 880.9748 (calcd. for $C_{36}H_{30}{}^{79}Br_2{}^{81}BrN_6O_6$, 880.9753), 882.9741 (calcd. for $C_{36}H_{30}{}^{79}Br\ {}^{81}Br_2N_6O_6$, 882.9732), 884.9692 (calcd. for $C_{36}H_{30}{}^{81}Br_3N_6O_6$, 884.9712). The NMR signal for C-4′ were observed in a spectrum acquired in H_2O/D_2O 9:1. The signal for H-4′ was obscured by NMR solvent.

4.4. Biological Assays

4.4.1. Antitumour Cytotoxicity

Protocols of testing at the DTP, NCI have been described elsewhere [24,25].

4.4.2. Antiparasitic and L6 Cytotoxicity Assays

Detailed protocols for these assays have been described elsewhere [26].

Supplementary Materials: The following are available online at http://www.mdpi.com/1660-3397/18/8/404/s1, Figure S1–S29: NMR spectra of compounds **4**–**8**.

Author Contributions: Design of the work, B.R.C. and M.M.C.; reactions, C.F.C.L. and M.M.C.; extraction and purification of natural product, C.F.C.L.; Writing original manuscript, B.R.C., M.M.C. and C.F.C.L.; Editing, B.R.C. and M.M.C.; Supervision, B.R.C. All authors have read and agreed to the published version of the manuscript.

Funding: This research received no external funding.

Acknowledgments: We acknowledge funding from the University of Auckland. We thank M. Kaiser (Swiss TPH) for parasite assay results, NCI DTP branch for testing compounds against the NCI-60 human tumour cell line panel, and M. Schmitz, R. Imatdieva and T. Chen for assistance with NMR and MS data acquisition.

Conflicts of Interest: The authors declare no conflict of interest.

References

1. Antunes, E.M.; Copp, B.R.; Davies-Coleman, M.T.; Samaai, T. Pyrroloiminoquinone and related metabolites from marine sponges. *Nat. Prod. Rep.* **2005**, *22*, 62–72. [CrossRef] [PubMed]
2. Hu, J.-F.; Fan, H.; Xiong, J.; Wu, S.-B. Discorhabdins and Pyrroloiminoquinone-Related Alkaloids. *Chem. Rev.* **2011**, *111*, 5465–5491. [CrossRef] [PubMed]
3. Perry, N.B.; Blunt, J.W.; McCombs, J.D.; Munro, M.H.G. Discorhabdin C, a highly cytotoxic pigment from a sponge of the genus *Latrunculia*. *J. Org. Chem.* **1986**, *51*, 5476–5478. [CrossRef]
4. Perry, N.B.; Blunt, J.W.; Munro, M.H.G. Cytotoxic pigments from New Zealand sponges of the genus *Latrunculia*: Discorhabdin A, discorhabdin B and discorhabdin C. *Tetrahedron* **1988**, *44*, 1727–1734. [CrossRef]
5. Li, F.; Janussen, D.; Tasdemir, D. New discorhabdin B dimers with anticancer activity from the Antarctic deep-sea sponge *Latrunculia biformis*. *Mar. Drugs* **2020**, *18*, 107. [CrossRef] [PubMed]
6. Li, F.; Pandey, P.; Janussen, D.; Chittiboyina, A.G.; Ferreira, D.; Tasdemir, D. Tridiscorhabdin and didiscorhabdin, the first discorhabdin oligomers linked with a direct C–N bridge from the sponge *Latrunculia biformis* collected from the deep sea in Antarctica. *J. Nat. Prod.* **2020**, *83*, 706–713. [CrossRef]
7. Zou, Y.; Hamann, M.T. Atkamine: A new pyrroloiminoquinone scaffold from the cold water Aleutian Islands *Latrunculia* sponge. *Org. Lett.* **2013**, *15*, 1516–1519. [CrossRef]
8. Zou, Y.K.; Wang, X.J.; Sims, J.; Wang, B.; Pandey, P.; Welsh, C.L.; Stone, R.P.; Avery, M.A.; Doerksen, R.J.; Ferreira, D.; et al. Computationally assisted discovery and assignment of a highly strained and PANC-1 selective alkaloid from Alaska's deep ocean. *J. Am. Chem. Soc.* **2019**, *141*, 4338–4344. [CrossRef]
9. Li, F.; Peifer, C.; Janussen, D.; Tasdemir, D. New discorhabdin alkaloids from the Antarctic deep-sea sponge *Latrunculia biformis*. *Mar. Drugs* **2019**, *17*, 439. [CrossRef]
10. Goey, A.K.L.; Chau, C.H.; Sissung, T.M.; Cook, K.M.; Venzon, D.J.; Castro, A.; Ransom, T.R.; Henrich, C.J.; McKee, T.C.; McMahon, J.B.; et al. Screening and biological effects of marine pyrroloiminoquinone alkaloids: Potential inhibitors of the HIF-1α/p300 interaction. *J. Nat. Prod.* **2016**, *79*, 1267–1275. [CrossRef]
11. Harris, E.M.; Strope, J.D.; Beedie, S.; Huang, P.A.; Goey, A.K.L.; Cook, K.; Schofield, C.J.; Chau, C.H.; Cadelis, M.M.; Copp, B.R.; et al. Preclinical evaluation of discorhabdins in antiangiogenic and antitumor models. *Mar. Drugs* **2018**, *16*, 241. [CrossRef] [PubMed]
12. Ford, J.; Capon, R.J. Discorhabdin R: A new antibacterial pyrroloiminoquinone from two Latrunculiid marine sponges, *Latrunculia* sp. and *Negombata* sp. *J. Nat. Prod.* **2000**, *63*, 1527–1528. [CrossRef] [PubMed]
13. Na, M.; Ding, Y.; Wang, B.; Tekwani, B.L.; Schinazi, R.F.; Franzblau, S.; Kelly, M.; Stone, R.; Li, X.-C.; Ferreira, D.; et al. Anti-infective discorhabdins from a deep-water Alaskan sponge of the genus *Latrunculia*. *J. Nat. Prod.* **2010**, *73*, 383–387. [CrossRef] [PubMed]

14. Jeon, J.-E.; Na, Z.; Jung, M.; Lee, H.-S.; Sim, C.J.; Nahm, K.; Oh, K.-B.; Shin, J. Discorhabdins from the Korean marine sponge *Sceptrella* sp. *J. Nat. Prod.* **2010**, *73*, 258–262. [CrossRef] [PubMed]
15. Wada, Y.; Harayama, Y.; Kamimura, D.; Yoshida, M.; Shibata, T.; Fujiwara, K.; Morimoto, K.; Fujioka, H.; Kita, Y. The synthetic and biological studies of discorhabdins and related compounds. *Org. Biomol. Chem.* **2011**, *9*, 4959–4976. [CrossRef] [PubMed]
16. Lam, C.F.C.; Grkovic, T.; Pearce, A.N.; Copp, B.R. Investigation of the electrophilic reactivity of the cytotoxic marine alkaloid discorhabdin B. *Org. Biomol. Chem.* **2012**, *10*, 3092–3097. [CrossRef]
17. Lam, C.F.C.; Cadelis, M.M.; Copp, B.R. Exploration of the influence of spiro-dienone moiety on biological activity of the cytotoxic marine alkaloid discorhabdin P. *Tetrahedron* **2017**, *73*, 4779–4785. [CrossRef]
18. Perry, N.B.; Blunt, J.W.; Munro, M.H.G.; Higa, T.; Sakai, R. Discorhabdin D, an antitumor alkaloid from the sponges *Latrunculia brevis* and *Prianos* sp. *J. Org. Chem.* **1988**, *53*, 4127–4128. [CrossRef]
19. Grkovic, T.; Pearce, A.N.; Munro, M.H.G.; Blunt, J.W.; Davies-Coleman, M.T.; Copp, B.R. Isolation and characterization of diastereomers of discorhabdins H and K and assignment of absolute configuration to discorhabdins D, N, Q, S, T, and U. *J. Nat. Prod.* **2010**, *73*, 1686–1693. [CrossRef]
20. Reich, H.J.; Jautelat, M.; Messe, M.T.; Weigert, F.J.; Roberts, J.D. Nuclear magnetic resonance spectroscopy. carbon-13 spectra of steroids. *J. Am. Chem. Soc.* **1969**, *91*, 7445–7454. [CrossRef]
21. Cadelis, M.M.; Copp, B.R. Investigation of the electrophilic reactivity of the biologically active marine sesquiterpenoid onchidal and model compounds. *Beilstein J. Org. Chem.* **2018**, *14*, 2229–2235. [CrossRef] [PubMed]
22. Davis, R.A.; Buchanan, M.S.; Duffy, S.; Avery, V.M.; Charman, S.A.; Charman, W.N.; White, K.L.; Shackleford, D.M.; Edstein, M.D.; Andrews, K.T.; et al. Antimalarial activity of pyrroloiminoquinones from the Australian marine sponge *Zyzzya* sp. *J. Med. Chem.* **2012**, *55*, 5851–5858. [CrossRef] [PubMed]
23. Copp, B.R.; Fulton, K.F.; Perry, N.B.; Blunt, J.W.; Munro, M.H.G. natural and synthetic derivatives of discorhabdin C, a cytotoxic pigment from the New Zealand sponge *Latrunculia* cf. *bocagei*. *J. Org. Chem.* **1994**, *59*, 8233–8238. [CrossRef]
24. Shoemaker, R.H. The NCI60 human tumour cell line anticancer drug screen. *Nat. Rev. Cancer* **2006**, *6*, 813–823. [CrossRef]
25. Malhotra, S.V.; Kumar, V.; Velez, C.; Zayas, B. Imidazolium-derived ionic salts induce inhibition of cancerous cell growth through apoptosis. *MedChemCommun* **2014**, *5*, 1404–1409. [CrossRef]
26. Orhan, I.; Sener, B.; Kaiser, M.; Brun, R.; Tasdemir, D. Inhibitory activity of marine sponge-derived natural products against parasitic protozoa. *Mar. Drugs* **2010**, *8*, 47–58. [CrossRef]